DETERMINATION OF THE DAMAGE PARAMETERS OF A SERIES 5000 ALUMINUM-MAGNESIUM ALLOY DURING SMALL PUNCH TEST

L.M.A. van Erp[1*], A. Díaz[2], R.H.J. Peerlings[1] and I.I. Cuesta[2]

[1] Department of Mechanical Engineering, University of Technology Eindhoven, De Zaale 5612AZ Eindhoven, The Netherlands.
[2] Grupo de Integridad Estructural, Universidad de Burgos, Avda. Cantabria s/n. 09006 Burgos, Spain
[*] Contact: l.m.a.v.erp@student.tue.nl

ABSTRACT

The Small Punch Test (SPT) is successfully established to indicate metallic material properties, it is predominantly used when the available material is limited and standard tests cannot be executed. During the SPT a fully constricted specimen in a die will be deformed by the use of spherical punch. One of the main objectives of this test is to assess fracture properties, a commonly used model is the Gurson-Tvergaard-Needleman (GTN) damage model. This model is widely used to simulate damage and failure, where void nucleation, coalescence and growth are taken into account . In this paper an assessment of the GTN parameters is elaborated, which can be utilized for further use of a 5000 series aluminum-magnesium alloy. The damage framework is determined by fitting the experimental force-displacement curve of different dog-bone-shaped specimens. Future work will be done on crack propagation using the estimated parameter values, with the assessment of the fracture toughness as ultimate goal.

KEYWORDS: Small punch test, GTN damage model, fracture parameters, numerical damage modelling, dog-bone specimens

INTRODUCTION

Nowadays, there is a high demand on environmental friendly policy regarding material consumption, since not all materials are limitless available. To save material, the testing method SPT (small punch test) is introduced in the recent decades. During the test a small specimen (typically 10x10x0.5 mm) is deformed with the use of a high-strength punch. The samples are embedded in a lower- and upper die, and punched until fracture occurs. This results in a tip displacement as a function of the applied load on the specimen. Small punch tests (SPT) are widely used in characterization of materials, this mechanical testing procedure provides properties when there is only a small amount of available material as an alternative for conventional fracture tests [1-3]. Especially the nuclear industry deals with limited availability of materials, therefore the used specimens have typical dimensions of 10x10x0.5 mm. These samples are clamped into a lower and upper die, where after a spherical indenter applies a force under displacement control, i.e. fixing the displacement rate, in the perpendicular direction.

Since the data cannot be extracted directly from the SPT, experiments are carried out. One of the main properties that can be numerically deduced from the force-displacement curve, are the coefficients for the Gurson-Tvergaard-Needleman (GTN) damage model. Taking into account the different material stages, from elastic until failure by means of nucleation, growth and coalescence of microvoids. Simulations with this model give insight in a better understanding of damage and failure of materials.

In this paper, the application of the GTN model is elaborated based on experimental force-displacement curves. Whereby the whole spectrum of damage, including void nucleation, growth and coalescence, is modeled to simulate the numerical curves, following a methodology provided by Cuesta et. al. [4].

EXPERIMENTAL METHODOLOGY

A typical experimental SPT setup is schematically shown in Figure 1. Here D_d, the lower die hole, is 4 mm. d_p is the diameter of the punch and equal to 2.5 mm. Furthermore, fillet radius r is 0.5 mm.

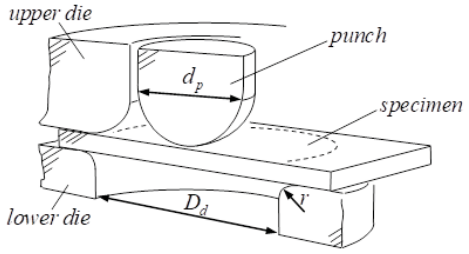

Figure 1. Schematic experimental setup of the SPT.

Examples of dog-bone-specimens can be seen in Figure 2. These samples are embedded and fully fixed between two bodies. Where after they are used to analyze the mechanical behavior for different confinement levels. In order to do this an isotropic materials is commonly used. The material selected for the specimens is aluminum, whereas the punch, lower- and upper-die are made out of steel. Whereby, a friction coefficient, μ between the different materials is used and equal to 0.21 [5]. The punch deforms the sample until fracture occurs by a displacement controlled experiment, typically with a drop rate of 0.5 mm/min.

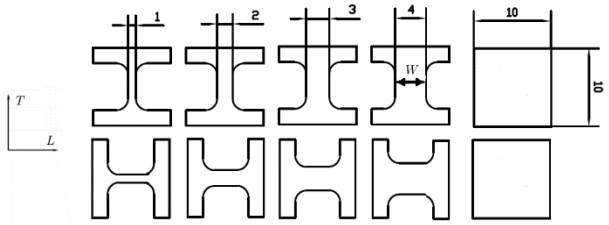

Figure 2. Samples for the SPT, using the different orientations L and T.

NUMERICAL METHODOLOGY

During this research, Abaqus CAE [6] was used in order to simulate a small punch test. It has been chosen to model a half of the specimen in three dimensions, to include irregularities for later research. During the analysis a mesh size of 0.1 mm is chosen in agreement with computation time and accuracy, since the reaction force in the punch barely depends on the mesh size. The samples are modeled with both symmetry boundary condition perpendicular to the thickness direction and fully constrained edges representing the embedded sample in the die. Moreover, the punch, upper and lower die are represented by means of an analytical 3D rigid body and modeled as a sphere and toroid respectively. Since the damage model can only be used in an explicit dynamic time step, the simulations were in a displacement controlled manner. Where the punch is forced to move -2.2 mm equally divided during the time step.

MATERIAL DESCRIPTION

During the SPT, the force *F* is measured as a function of the punch tip displacement δ, Figure 3 shows a typical behavior of this curve. As can be seen, there are six stages that can be distinguished. These stages will provide information about necessary parameters;

- Stage I: Elastic behavior.
- Stage II: This stage shows the transition between elastic and plastic behavior.
- Stage III: The material undergoes pure plastic behavior.
- Stage IV: Here the maximum load is reached and the specimen undergoes a change in thickness.
- Stage V: In this stage the material shows softening phenomena and cracks will grow.
- Stage VI: Final failure stage, the punch has penetrated through the specimen. Usually, the test is stopped now.

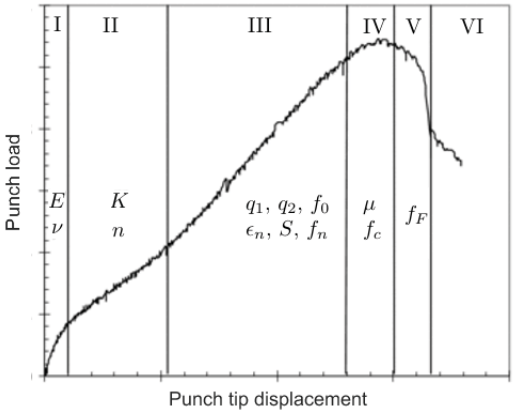

Figure 3. Typical force-displacement curve for a SPT, with the parameters indicating the different stages [4].

In this work, a series 5000 aluminum-magnesium alloy is investigated. Due to its isotropic and elastic nature, the material behavior in stage I is described by Hooke's Law with *E* and *v*, the Young's modulus and Poisson ratio respectively, as representing parameters.

For larger punch tip displacement the second stage is entered. Here, *K* and *n*, the strength coefficient and strain hardening exponent, play an important role to describe the behavior. Often the plasticity is fitted by a Hollomon-type equation, denoted by Equation (1).

$$\sigma = K\epsilon_p^n \tag{1}$$

This equation is used to extrapolate the stress-strain curve in the plastic regime. This methodology consists of a chosen interval where the material does not undergo damage. Furthermore, ϵ_p is the plastic strain and can be computed using the stress at point *i*, σ_i using:

$$\epsilon_p = \epsilon - \frac{\sigma_i}{E} \tag{2}$$

However, this is not enough to describe the materials behavior until fracture. A commonly used model to define damage in a continuum medium is the Gurson-Tvergaard-Needleman (GTN) model. It predicts damage by including porosity, nucleation, growth and coalescence of voids. Herewith, the stages III, IV and V can be closed and the full force-displacement can be

defined. The GTN damage model is mathematically denoted as: [7,8]

$$Q = \left(\frac{\bar{\sigma}}{\sigma_*}\right)^2 + 2q_1 f^* \cosh\left(\frac{q_2\sigma_{kk}}{2\sigma_*}\right) - [1 + (q_1 f^*)^2] = 0 \quad (3)$$

In this equation is σ_{kk} the first invariant of the stress state, $\bar{\sigma}$ the Von Mises equivalent stress and σ_* the flow stress of the matrix. To account for hydrostatic stress effects for all strain levels, model coefficient q_1 and q_2 are introduced. Furthermore, f^* is the modified porosity which accounts for a decrease in load due to void coalescence:

$$f^* = \begin{cases} f & if\ f \le f_c \\ f_c + \delta(f - f_c) & if\ f > f_c \end{cases} \quad (4)$$

Where, f the void volume fraction, f_c the critical porosity. In Stage IV, f_c is the most dominant parameter. At f_c, the interaction and coalescence between voids starts with rate δ_*. To determine δ_*, the next ratio can be used:

$$\delta_* = \frac{f_u^* - f_c}{f_F - f_c} \quad (5)$$

Stage V is influenced by f_F, the critical volume void fraction when the material fails, and f_u^* is equal to $1/q_1$. High strains lead to an increase of porosity due to several influences. δ_* determines the decrease after the maximum load is reached in this stage. In Stage III first, the existing microvoids will grow, this results in an increase of f. This results in a linear regime in the force-displacement curve because of the large plastic strains and voids grow together with the punch displacement. Secondly, new voids are generated as a consequence of the greater plastic strains. These phenomena can be expressed as:

$$\dot{f} = \dot{f}_{growth} + \dot{f}_{nucleation} \quad (6)$$

With

$$\dot{f}_{growth} = (1 - f)\dot{\epsilon}_{kk}^p \quad (7)$$

$$\dot{f}_{nucleation} = \frac{f_N}{S\sqrt{2\pi}} exp\left[-\frac{1}{2}\left(\frac{\epsilon_m^p - \epsilon_n}{S}\right)^2\right]\dot{\epsilon}_m^p \quad (8)$$

$\dot{\epsilon}_{kk}^p$ is the plastic strain increment tensor, the trace of this tensor controls the void growth. The nucleation of voids depends on f_N, which is the void volume nucleation fraction and ϵ_n the strain at which nucleation starts. S is the standard deviation of ϵ_n; if S is relatively low the material is considered as homogeneous. Finally, f_0 is the initial void volume fraction.

METHODOLOGY FOR MATERIAL PARAMETERS

Different parameters can be extracted from the force-displacement curve by observing the several stages in the fracture process. The parameters of interest on the one hand depend on the isotropic behavior of the material and on the other hand on the triaxiality. However, not all data can be directly extracted from this curve. In order to assign values to the first two stages conventional tensile tests are examined, using tensile bars of the same type of aluminum. Results are shown in Figure 4. Here, different orientations (L and T) of the aluminum are considered to account for possible anisotropy.

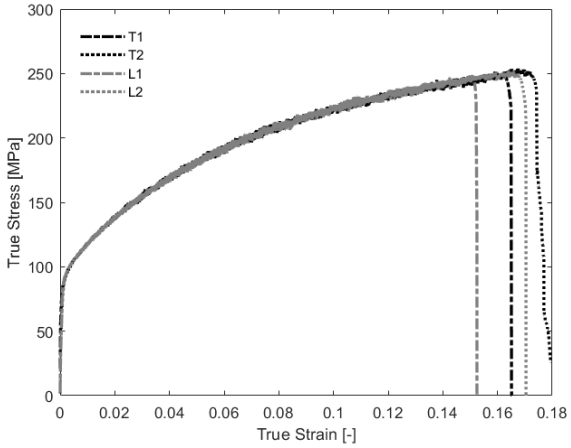

Figure 4. Stress as a function of strain during tensile test, with L and T the different orientation of the aluminum specimens.

From this curve the elastic-plastic behavior can be described, where it becomes necessary to extrapolate the stress strain curve with a Hollomon-type equation (1). The first two stages can now be defined by the values given in Table 1.

Table 1. Elastic-plastic behavior parameters.

E (MPa)	v	K	n
70000	0.334	415.5	0.2755

Next, the Gurson-Tvergaard-Needleman damage model is widely used to simulate fracture behavior. The model represents stage III, IV and V, where a combination of numerical and experimental data is required to obtain the parameters that fit the force-displacement curve. However, other studies prove that q_1=1.5, q_2=1.0 are typical values for metals [6-8]. Parameter S depends on the homogeneity of the material so a value of S=0.1 [9] is sufficient for the simulations. Furthermore, it is assumed that there are no initial voids in the specimens, so f_0 is chosen to be zero. Additionally, the kinematic friction coefficient for steel on aluminum is set to μ=0.21.

The determination of the void parameters for simulating a small punch test are following a methodology provided by Cuesta [4]. After the implementation of the plasticity model, excluding the damage GTN model, the numerical force-displacement curve for SPT follows the first stages properly as shown in Figure 5.

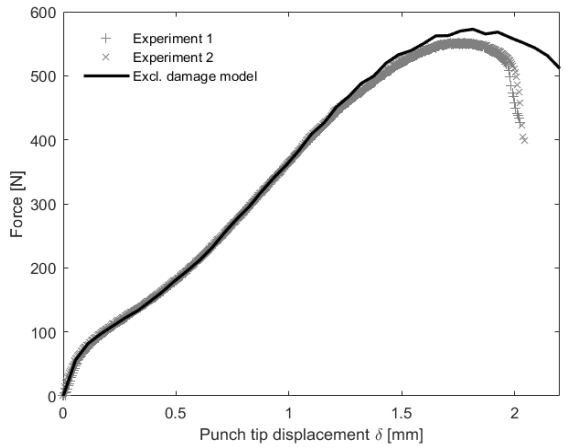

Figure 5. Experimental force-displacement curve for a SPT, with the numerical test excluding a damage model.

In order to control the curvature in stage III and IV, a variation of parameters ϵ_N and f_N governs the shape. Figure 6 shows the influence of increasing f_N on the graph. Here, the values for f_N are chosen on the interval [0.0, 0.03] in 0.005 increments. As observed, the curvature of the graph changes for increasing f_N. Noticeable is that changes in ϵ_n on typical interval [0.0, 0.2] in 0.1 increments have negligible influence on the curve compared with f_N.

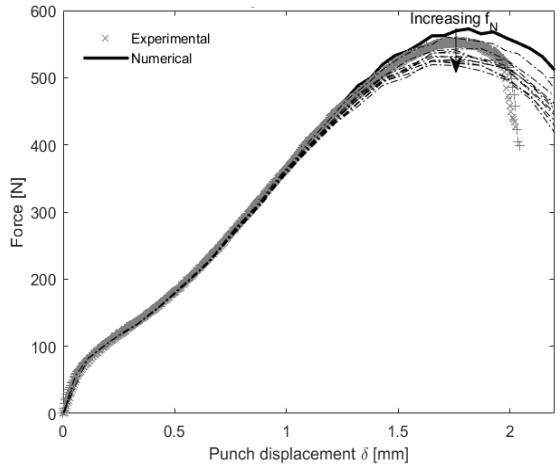

Figure 6. Experimental force-displacement curve for a SPT with the numerical test, including a range of the first two parameters of the damage model ϵ_n and f_N.

Simulations show that for ϵ_n=0.1 and f_N=0.01 the numerical curve fits the experimental curve reasonably, as can be seen in Figure 7. Compared with the plasticity model, the maximum allowable force is lowered. Since critical parameters for void fraction are not included, no fracture is observed yet. Therefore, the deviation of the curve starts at displacement δ=1.9 mm. This point marks the initiation of the void coalescence.

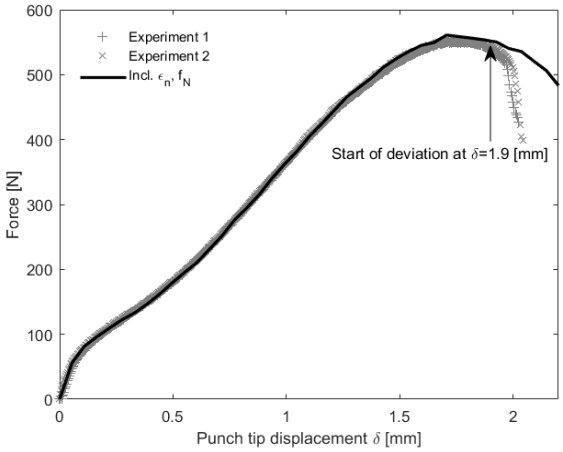

Figure 7. Experimental force-displacement curve for a SPT with the numerical test, including the first two parameters of the damage model with ϵ_n=0.1 and f_N=0.01.

The force-displacement curve has now entered stage IV. Here, the specimen reduces its thickness. This is determined by parameter f_c, which can be valued by looking at the total void volume fraction. In Figure 8 the void volume fraction as a function of tip displacement is shown. It is observed that for a displacement δ=1.9 mm the failure zone starts to be visible. The corresponding critical void volume fraction is equal to f_c= f(δ=1.9)=0.06.

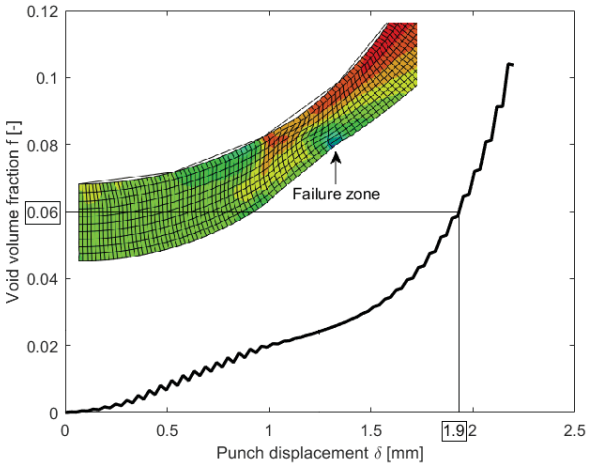

Figure 8. Void volume fraction f as a function of punch displacement δ, with the initiation of the failure zone and computation of critical void parameter f_c.

After the critical void fraction, the fracture will start and the curve is governed by f_F. The fracture volume fraction represents the decreasing slope in the force-displacement curve after fracture occurs. As observed in Figure 9, the curve changes for decreasing values for f_F. This can be used to control the cut-off point after the maximum load.

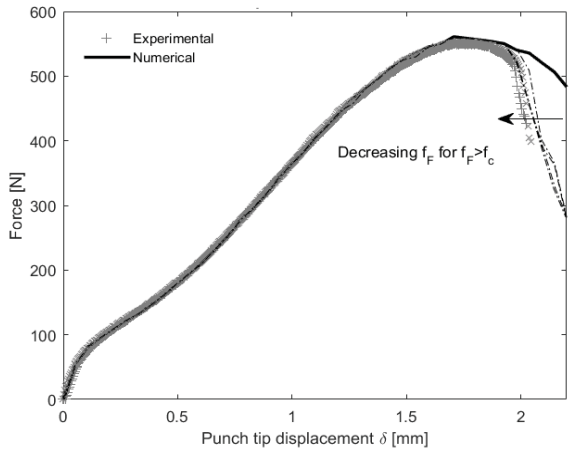

Figure 9. Experimental force-displacement curve for a SPT, with the numerical test including all the parameters of the damage model ϵ_n, f_N, f_c and decreasing failure void fraction f_F.

In Figure 10, the numerical simulation and experimental data match in every stage for the total GTN damage model with f_c=0.06 and f_F =0.07. Altogether, an overview of the damage parameters for a series 5000 aluminum-magnesium alloy is given in Table 2.

Table 2. GTN damage model parameters.

q_1	q_2	f_0	S	ϵ_n	f_N	f_c	f_F
1.5	1.0	0	0.1	0.1	0.01	0.06	0.07

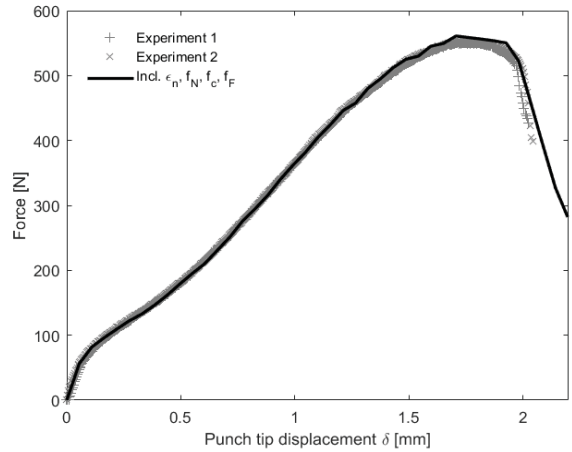

Figure 10. Experimental force-displacement curve for a SPT, with the numerical test including all the parameters of the damage model ϵ_n=0.1, f_N=0.01, f_c=0.06 and f_F=0.07.

Since the GTN damage model depends on the triaxiality of the specimen, this implies that for each sample the methodology must be repeated and different parameters might be found for each geometry. This is done for the dog-bone specimens with different sample widths *W*. Results are shown in Figure 11; here a good agreement between experimental and numerical data is observed. In Table 3 the governing values for the different samples sizes are given. As can be seen the value for f_N is constant, f_c and f_F increase for increasing sample width.

Figure 12 shows the tested samples with different widths. In order to employ failure behavior, the samples are analyzed using a scanning electron microscope (SEM). In these SEM images, there are different failure modes observed. For a sample width of *W*=10 mm the crack has propagated circumferentially, where for other widths the crack in centered in the middle and is almost horizontal. In *W*=3 mm specimens, the material has started to neck in the center. *W*=1 and *W*=2 a more brittle behavior is observed since these specimens exhibit a more uni-directional elongation.

Table 3. GTN model void fraction parameters for different sample widths.

	f_N	f_c	f_F
W=1 mm	0.01	0.015	0.02
W=2 mm	0.01	0.025	0.03
W=3 mm	0.01	0.03	0.04
W=4 mm	0.01	0.03	0.04
W=10 mm	0.01	0.06	0.07

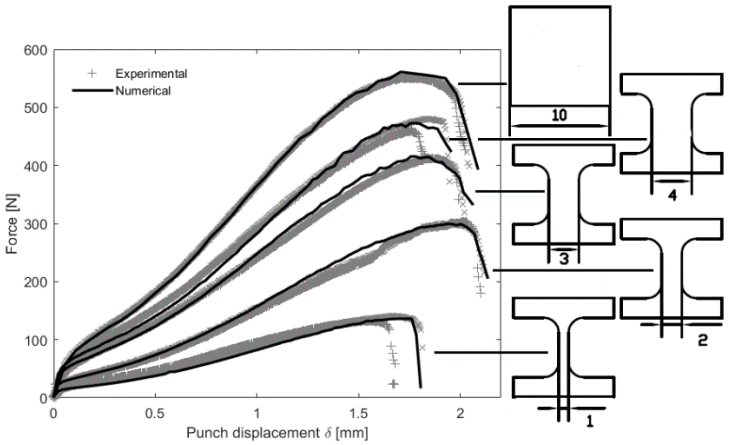

Figure 11. Numerical force-displacement curve for SPT with different sample widths.

CONCLUSIONS

To identify the damage properties in a material to use for numerical simulation, a methodology for the determination is necessary. With the use of the Gurson-Tvergaard-Needleman model a good approximation of the force-displacement curve was obtained, since this model reproduces the behavior throughout the different stages. Using this methodology it is possible to determine the material parameters using a squared aluminum-magnesium alloy plate by means of a correlation between numerical and experimental data. However, since the GTN parameters strongly depend on the specimens triaxiality, a repetition for different samples is necessary.

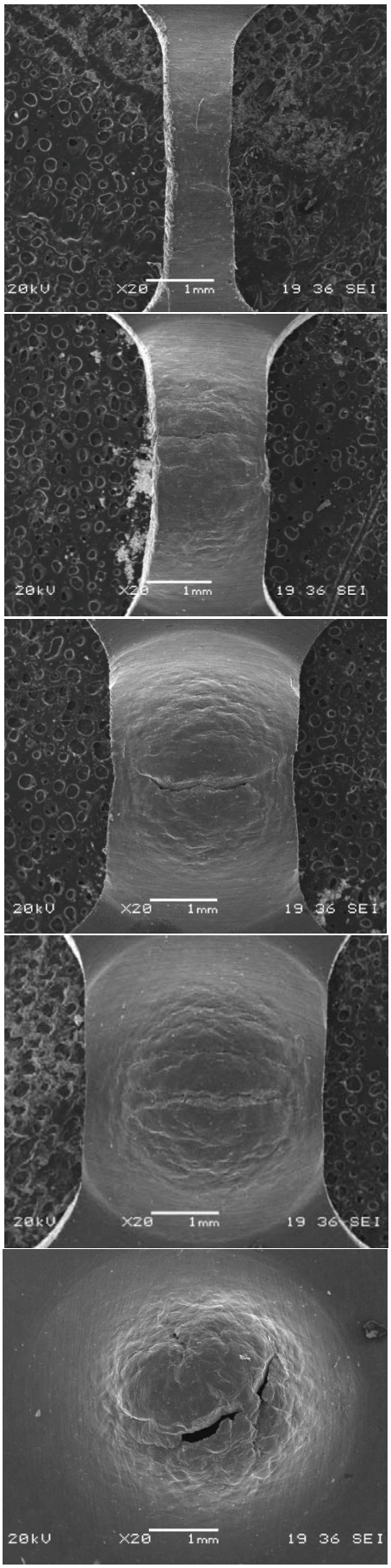

Figure 12. Tested samples with different widths.

ACKNOWLEDGMENTS

The authors wish to thank the funding received from the Ministry of Education of the Regional Government of Castile and Leon under the auspices of the support for the Recognized Research Groups of public universities of Castile and Leon started in 2018, Project: BU033G18

REFERENCES

[1] Ha, J.S. and Fleury, E. (1998) Small Punch test to estimate the mechanical properties of steels for steam power plant: I mechanical strength. *int. J. Press. Vess. Pip.* **75**, 699-706.

[2] Ha, J.S. and Fleury, E. (1998) Small Punch test to estimate the mechanical properties of steels for steam power plant: II mechanical strength. *int. J. Press. Vess. Pip.* **75**, 707-713.

[3] Campitelli, E., et al. (2004) Assessment of the constitutive properties from small ball punch test: Experiment and modelling, *J. Nucl. Mater.* **335**, 366-378.

[4] Cuesta, I.I., Alegre, J.M. and Lacalle, R. (2010) Determination of the Gurson-Tvergaard damage model parameters for simulating small punch tests. *Fatigue Fract Engng Mater Struct* **33**, 703-713.

[5] Chaplin, R.L. and Chilson, P.B. (1986) The coefficient of kinetic friction for aluminum, Clemson, *Wear* **107**, 213-225.

[6] Abaqus/CAE 6.14 (2014) user's manual , *SIMULIA web site*. Dassault Systèmes.

[7] Abenndroth, M and Kuna, M. (2003) Determination of deformation and failure properties of ductile materials by means of the small punch test and neural networks. *Comput. Mater. Sci.* **28**, 633-644.

[8] Autillo, J., et al. (2006) Utilizacion del ensayo miniatura de punzonamiento (Small Punch Test) en la caracterizacion mecanica de aceros. *Anales de Mecanica de Fractura* **I**, 77-83.

[9] Teng B, Wang W, Liu Y, Yuan S. (2014) Bursting prediction of hydroforming aluminium alloy tube based on Gurson-Tvergaard-Needleman damage model. *Procedia Engineering* **81**, 2211-6.